

The Influence of the Substrate Material on the Structure and Electrophysical Properties of $\text{Ba}_x\text{Sr}_{1-x}\text{TiO}_3$ Thin Films

M. S. Afanas'ev^a, D. A. Kiselev^{a, b, *}, S. A. Levashov^a, V. A. Luzanov^a, A. Nabihev^c,
V. G. Naryshkina^a, A. A. Sivov^a, and G. V. Chucheva^a

^a Fryazino Branch of Kotel'nikov Institute of Radio Engineering and Electronics, Russian Academy of Sciences,
Fryazino, Moscow oblast, 141190, Russia

^b National University of Science and Technology MISiS, Moscow, 119049, Russia

^c Azerbaijan State Pedagogic University, Baku, 370000, Azerbaijan

*e-mail: dm.kiselev@gmail.com

Received November 8, 2017

The high-frequency spraying method has been used to produce $\text{Ba}_x\text{Sr}_{1-x}\text{TiO}_3$ thin films on (111)Pt/(100)Si and SiO_x /(100)Si substrates. The synthesized films have proven to be single-phase with a polycrystalline structure. In this paper, we show the influence of the platinum sublayer on such parameters as roughness, mean size of grains, and the local polarization of $\text{Ba}_x\text{Sr}_{1-x}\text{TiO}_3$ thin films. Possible mechanisms of the obtained results related to the intragrain conductivity and the nature of interaction of a ferroelectric film with its substrate are discussed.

DOI: 10.1134/S1063783418050025

1. INTRODUCTION

Heterostructures engaging thin ferroelectric films as dielectrics are of special interest in connection with their potential use to create a new generation of the element basis of the state-of-the-art electronics, in particular, nonvolatile reprogrammable storage devices and tunable high-capacity condensers [1, 2]. At present, intensive studies of heterostructures using thin $\text{Ba}_x\text{Sr}_{1-x}\text{TiO}_3$ ferroelectric films [3–5] are ongoing.

The purpose of this paper is to study the effect produced by the substrate material on the structure and electrophysical properties of thin ferroelectric films composed of $\text{Ba}_x\text{Sr}_{1-x}\text{TiO}_3$ (BST).

2. PRODUCTION AND EXAMINATION

The ferroelectric films were produced using the method of high-frequency atomization of a ceramic target at the PLASMA-50SE test facility. The construction and description of the facility are presented in [6]. The films were deposited by ceramic target atomization in a low-temperature oxygen plasma (O_2) to provide the target component transition to the gas phase (film-forming medium) with the film-forming medium subsequent condensation on a substrate. The procedure of film deposition was as follows. A 10 × 10 mm substrate was fixed on a heater using a 0.3-mm thick stainless steel holder. The working chamber was

sealed. The chamber was depressurized using NVR-16 DM forepump to a residual pressure of 1.0 Pa. Then medically pure oxygen was supplied to the chamber to raise the pressure to 60.0 Pa. The residual pressure was monitored automatically by a system of RGG-3 gas discharge regulator with an accuracy of +0.01 Pa. The substrate temperature was monitored and maintained automatically by means of TRM-101 microprocessor meter with an accuracy of +5°C. The substrate was heated to 400°C and kept at this temperature for 15 min. Then the power module of HF generator was started and oxygen HF plasma was ignited in the enclosed volume.

The procedure of film production included two stages. The first stage presumed the procedure of deposition in the oxygen plasma. At the second stage, the deposited film was subject to a treatment in the oxygen environment. For this purpose, the HF generator was switched off, the vacuum valve was closed, and the pressure of oxygen in the chamber was raised to 100 Pa. Then the substrate was cooled to the ambient temperature over 2 h. The deposition of ferroelectric films lasted for 30 min, the oxygen working pressure was 60 Pa, the cathode–anode power was 290 W, and the substrate temperature during the deposition was 620°C.

Finally, thin BST films on (111)Pt/(100)Si and SiO_x /(100)Si substrates were produced. The HF plasma optical radiation was monitored during the film formation. The measuring technique is described

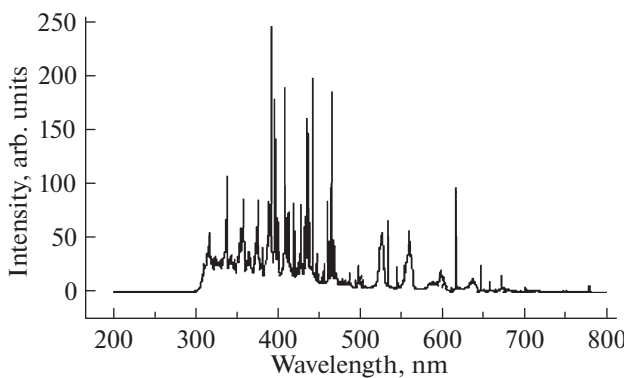


Fig. 1. Plasma radiation spectrum.

in [7]. The radiation was registered by MDR-23 monochromator with FEU-100 in the range of 200–800 nm.

The film phase composition was analyzed using a D8 Discover X-ray diffractometer (Bruker-AXS, Germany) in the collateral beam geometry. An X-ray tube with a copper anode (radiation $\text{Cu}K\alpha$) was taken as the X-ray source. The focus was linear. The beam width was 0.2 mm. The shooting was carried out at 40 kV–40 mA. The Goebel mirror was used to enhance the intensity of the primary beam and to achieve its partial monochromatization and collimation in the diffraction plane. No secondary monochromator was used. The measuring algorithm: 2θ–θ scanning with a step of 0.02, 1D LynxEye detector. The qualitative phase analysis engaged EVA software (Bruker-AXS) and ICDD databases in the PDF-2 format.

Volt-farad characteristics (VFC) of heterostructures based on BST were measured at ambient temperature by a computerized device using high-precision LCR Agilent E4980A meter [8]. The measuring signal frequency was 100 kHz with an amplitude of 25 mV. The dependence of capacity C of Au/BST/ SiO_x /(100)Si (MDP structure) samples on the voltage of displacement varying from –20 V to +20 V (forward motion) and from +20 V to –20 V (reverse motion) in increments of 10 mV, and with reading speed of 3 point/s were recorded. For Au/BST/(111)Pt/(100)Si heterostructures (MDM structure), the displacement voltage varied from –10 V to +10 V and back with a step of 10 mV at the reading speed of 3 point/s.

The surface visualization, the process of local polarization, and recording signals of surface potential were carried out using a MFP-DTM Stand Alone scanning probe microscope (Asylum Research, USA) in semi-contact, contact (polarization process) modes, and the Kelvin probe method. Asytec-01 brand cantilevers were used for scanning. All measurements were performed at ambient temperature.

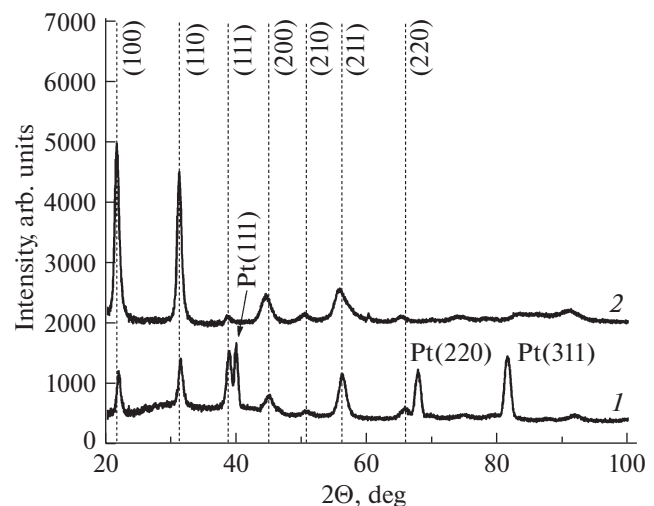


Fig. 2. Diffractograms of BST/(111)Pt/(100)Si (1) and BST/ SiO_x /(100)Si (2) heterostructures at ambient temperature.

3. EXPERIMENTAL RESULTS AND DISCUSSION

The spectrum of plasma radiation registered in the process of BST film deposition is presented in Fig. 1. It shows the spectrum prominent feature, which is the reproducibility of growing ferroelectric films with the given crystal chemical parameters.

In Fig. 2, the films synthesized on substrates of different types are shown; they are monophase and polycrystalline. Changes in correlations of the peak intensities as compared to the bar chart, apparently, indicate the process of texture formation. The data obtained using the diffraction analysis show that the film composition is $\text{Ba}_{0.6}\text{Sr}_{0.4}\text{TiO}_3$. At the same time, the BST film synthesized on a platinized silicon substrate displays the equal intensity of reflexes (Fig. 2, curve (1), which allows us to speak about the “inheritance” by the substrate of orientation in the process of BST film synthesis.

The measured VFC of the MDM structure are presented in Fig. 3, curve (1). The capacity obtained varies from 350 pF to 550 pF. The VFC curve is symmetrical in relation to abscissa and slightly resembles a negative quadratic function with its maximum capacity at 0 V. When the displacement voltage reaches –10 V and +10 V, the capacity attains the minimum of 350 pF. In the region of negative voltages, there is a low-grade hysteresis curve.

The capacity of MPD structure (Fig. 3, curve (2)) varies from 5.6 pF to 65 pF. The VFC curve displays a well pronounced hysteresis curve directed counter-clockwise; i.e., the left front of the loop corresponds to the voltage of forward displacement motion, and the right front to that of the reverse motion. The loop width is 8 V. The loop is asymmetric, its left and right

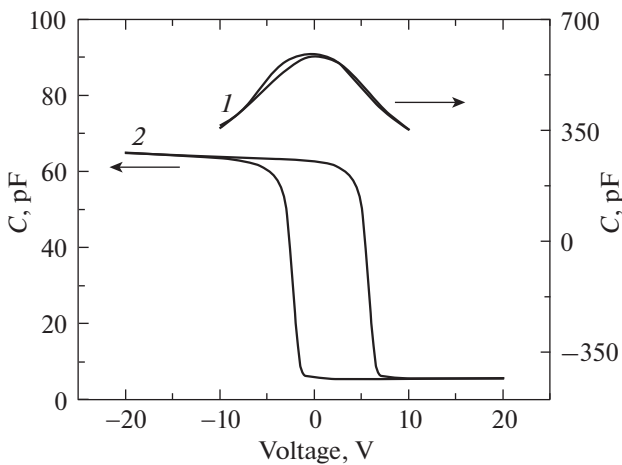


Fig. 3. Volt-farad characteristics of Au/BST/(111)Pt/(100)Si (1) and Au/BST/SiO_x/(100)Si (2) heterostructures.

fronts are parallel and rather steep, and its center is displaced toward the region of positive voltages.

The influence of the substrate type (material) on the degree of roughness of BST film surface was studied. In Fig. 4, surfaces of the studied heterostructures are imaged (scanning area $5 \times 5 \mu\text{m}^2$) obtained by the scanning probe microscope. The statistical analysis shows that the root-mean-square roughness of the surface is $r_{\text{ms}} = 4.9 \text{ nm}$ for BST/(111)Pt/(100)Si and $r_{\text{ms}} = 7.0 \text{ nm}$ for BST/SiO_x/(100)Si.

At the same time, the difference between average grain sizes (over the studied area of scanning) is observed: 60 nm for BST/(111)Pt/(100)Si and 95 nm for BST/SiO_x/(100)Si. Apparently, in the case of platinized silicon, BST grains have a columnar structure, which influences their lateral size. Hence, we can say that the material and, which is more important, the orientation of the substrate produce a direct influence on the degree of roughness of the surface, and on the mean size of a grain, which, in turn, affects the physical (electrophysical) properties (characteristics) of the BST films.

Studies of BST film local polarization were carried out using the methods of piezoresponse (piezometric) power microscopy and Kelvin probe. In Fig. 5, the residual surface potential of a section of BST film surface examined after preliminary polarization with application of $\pm 30 \text{ V}$ is imaged. The constant voltage was applied to a conductive probe of the atomic-power microscope that was in contact with the film surface, so that the parameters were “recorded” in one line under the impact of positive and negative voltage. The scans presented in Fig. 5 are of equal scale (contrast) along the Z axis and clearly show that the film deposited on a platinized substrate (Fig. 4a) displays a signal of magnitude (contrast) times less than the BST film synthesized on a silicic substrate (Fig. 5b).

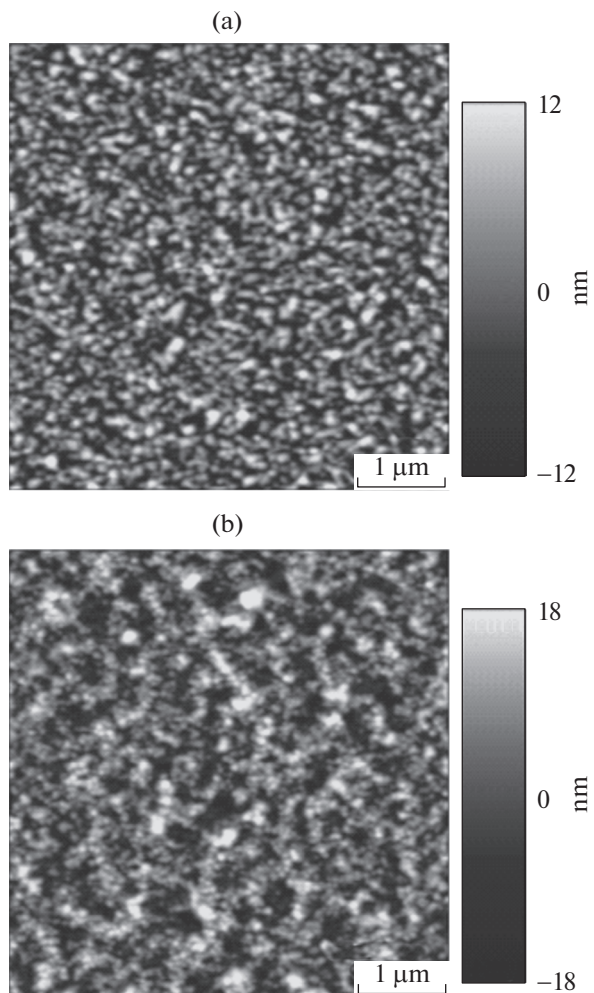


Fig. 4. AFM images of the surface geometry of BST film deposited on a platinized (a) and silicon (b) substrates.

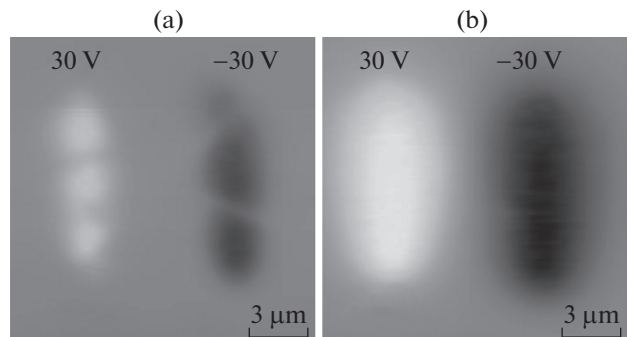


Fig. 5. Images of the residual surface potential of BST film deposited on a platinized (a) and a silicon (b) substrate, after the prepolarization.

This is confirmed by the profiles of surface potential distribution (Fig. 6, curves (1), (2)), plotted over the middle of the scanned regions presented in Fig. 5. The significant difference observed between the values of the residual potential on BST film surface can be

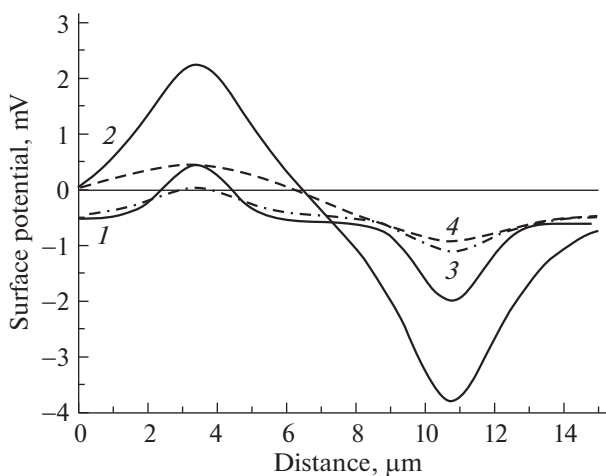


Fig. 6. The geometry of the residual surface potential for BST/(111)Pt/(100)Si ((1), (3)) and BST/SiO_x/(100)Si ((2), (4)). Curves (1), (2) are potential geometries observed immediately after polarization; curves (3), (4) are observed in a 30-min period after polarization (relaxation).

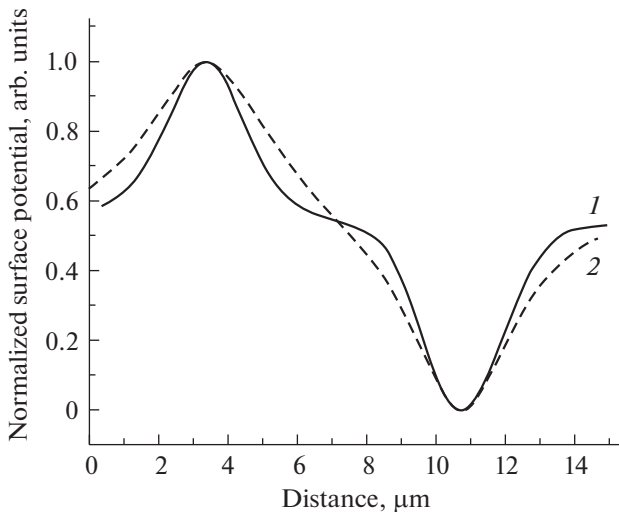


Fig. 7. Normalized signals of the residual potential for the studied samples: (1) is BST/(111)Pt/(100)Si, 2 is BST/SiO_x/(100) Si.

caused by different mechanisms of interaction of the ferroelectric materials and the lower electrode; in our case these are platinum and SiO_x. Additionally, the difference between the halfwidths of polarization lines of the studied samples is apparent from the normalized values of signals of the residual potential (Fig. 7). Thus, the halfwidths of lines polarized by constant voltage is wider for BST/SiO_x/(100)Si than for BST/(111)Pt/(100)Si, which might be connected with the conductivity of intragrain boundaries, and accumulation of a charge near the ferroelectric film–substrate interface. This hypothesis is supported by the fact that the polarized regions are less stable in time for BST samples synthesized on a silicon substrate. For

example, comparing curves (2), (4) in Fig. 6 we see that the magnitude of surface potential of polarized lines decreases 4–5-fold over 30 min for BST/SiO_x/(100)Si, while for the BST film synthesized on a platinized substrate, the decrease for the same period does not exceed 50% (curves (1), (3)).

4. CONCLUSIONS

Thin BST ferroelectric films were synthesized on two types of substrates materials using the method of high-frequency magnetron atomization. It is shown that the platinum underlayer influences roughness and mean size of grains of the studied BST film and its local polarization. The effective inductivities of the films synthesized on a silicon substrate with a platinum underlayer, and on a silicon substrate with a silicon oxide underlayer are 1240 and 135, respectively. It was discovered that the obtained structures are manageable. The studies showed that reprogrammable storage devices and reconfigurable condenser elements can be created based on these structures.

ACKNOWLEDGMENTS

This study was supported in part by the Russian Foundation for Basic Research (projects nos. 16-07-00665 and 16-07-00666) and by the Programs of Basic Researches of the Presidium of the Russian Academy of Sciences: Nanostructures: Physics, Chemistry, Biology: Engineering Principles.

The authors are grateful to M.I. Voronova for help in X-ray analysis of BST films.

REFERENCES

1. S. Kawashima and J. S. Cross, in *Embedded Memories for Nano-Scale VLSIs*, Ed. by K. Zhang (Springer Science, New York, 2009), p. 279.
2. K. A. Vorotilov, V. M. Mukhortov, and A. S. Sigov, *Integrated Ferroelectric Devices*, Ed. by A. S. Sigov (Energoatomiz, Moscow, 2011) [in Russian].
3. A. Queraltó, A. Pérez del Pino, M. de la Mata, J. Arbiol, M. Tristany, A. Gómez, X. Obradors, and T. Puig, *Appl. Phys. Lett.* **106**, 262903 (2015).
4. A. N. Kuskova, R. V. Gainutdinov, and O. M. Zhigalina, *J. Surf. Invest.: X-ray, Synchrotron, Neutron Tech.* **8**, 761 (2014).
5. X. B. Yan, X. L. Jia, T. Yang, J. H. Zhao, Y. C. Li, Z. Y. Zhou, and Y. Y. Zhang, *Phys. Lett. A* **380**, 3509 (2016).
6. M. S. Afanas'ev and M. S. Ivanov, *Phys. Solid State* **51**, 1328 (2009).
7. M. S. Afanas'ev, G. V. Chucheva, and A. E. Nabiev, *Phys. Solid State* **57**, 1377 (2015).
8. E. I. Goldman, S. A. Levashov, V. G. Naryshkina, and G. V. Chucheva, *Semiconductors* **51**, 1136 (2017).

Translated by N. Semenova